Neuron
Viewpoint

A Universal Property of Axonal and Dendritic Arbors

Joseph Snider,[1] Andrea Pillai,[1] and Charles F. Stevens[1,*]
[1]The Salk Institute, 10010 North Torrey Pines Road, La Jolla, CA 92037, USA
*Correspondence: stevens@salk.edu
DOI 10.1016/j.neuron.2010.02.013

SUMMARY

Axonal and dendritic arbors can be characterized statistically by their spatial density function, a function that specifies the probability of finding a branch of a particular arbor at each point in a neural circuit. Based on an analysis of over a thousand arbors from many neuron types in various species, we have discovered an unexpected simplicity in arbor structure: all of the arbors we have examined, both axonal and dendritic, can be described by a Gaussian density function truncated at about two standard deviations. Because all arbors are characterized by density functions with this single functional form, only four parameters are required to specify an arbor's size and shape: the total length of its branches and the standard deviations of the Gaussian in three orthogonal directions. This simplicity in arbor structure can have implications for the developmental wiring of neural circuits.

INTRODUCTION

One of neurobiology's central problems is how neural circuits form in development. But to even think about this problem we need to know how many parameters are needed to specify the form of an arbor. A typical vertebrate axonal arbor makes about 10^4 synapses, and a dendritic arbor receives about the same number. If the exact location of each synapse were important, that would mean at least 6×10^4 parameters (one each for the three coordinates specifying the synapse location for the neuron's axonal and dendritic arbors) would be required per arbor—actually the number would be larger because the assignment of synapses to arbor branches would be necessary. Given the large number of neurons in the brain, around 10^5 per microliter, this scheme would require a prohibitive amount of information, because at least 6×10^9 parameters would be required to wire a microliter volume of neuropil. To explore simpler ideas about neural network development than the brute force specification of each synapse position, we would need to know the smallest number of parameters needed to give a quantitative description of an arbor's form. This is the question we address here.

Each axonal arbor in the brain distributes information over some particular part of a neural circuit, a region called its "territory," and each dendritic arbor samples the information available in its territory. Discovering the structural principles that axons and dendrites use to distribute and sample information is central to understanding how neural circuits are constructed and how they operate. Here we describe a simple structural principle to which the arbors of both axons and dendrites conform: the density of arbor branches in space is described by a Gaussian that is truncated at around two standard deviations from the arbor center. Because all of the arbors we have studied are quantitatively characterized by the same type of function, only three parameters—the standard deviations in three directions—are needed to specify how the arbor is distributed spatially.

RESULTS

Strategy for Describing Arbor Structure

The details of arbor structure (Binzegger et al., 2004a; Uylings and van Pelt, 2002) are, of course, important, but one can also focus on the statistics of how arbor branches are distributed in space, because this distribution determines what circuits can possibly be formed (Binzegger et al., 2004b; Chklovskii, 2004; Hellwig, 2000; Kalisman et al., 2003; Krone et al., 1986; Liley and Wright, 1994; Lübke et al., 2003; Peters and Payne, 1993; Shepherd et al., 2005; Sholl and Uttley, 1953; Stepanyants et al., 2002; Stevens, 1982; Uttley, 1955). In order to characterize the structural basis for information distribution and collection, we have studied the arbor spatial density function, an example of which is illustrated in Figure 1A. In this figure, we show a goldfish two-dimensional retinotectal axon arbor, stained with DiI and reconstructed with Neurolucida (see Experimental Procedures), together with the arbor's spatial density estimated by placing a 6×6 grid over the arbor and adding up the branch lengths in each grid box. The density of arbor branches is highest near the center and declines systematically toward the edges of the arbor's territory.

To learn the properties of the arbor density function, we must compare this function across different types of arbors. The estimate of the arbor density function presented in Figure 1A is, however, rather crude and has insufficient spatial resolution to permit a detailed comparison of different arbors. One way to improve the spatial resolution for the estimate of arbor density might be to decrease the box size of the covering grid. But this approach will not work because most arbors, like the one illustrated in Figure 1A, are so sparse that estimates of density at better spatial resolution are too noisy to be useful. The usual way to improve the noisy estimate would be to average across arbors, but this approach is also unsatisfactory because we do not know in advance which arbors share the same density

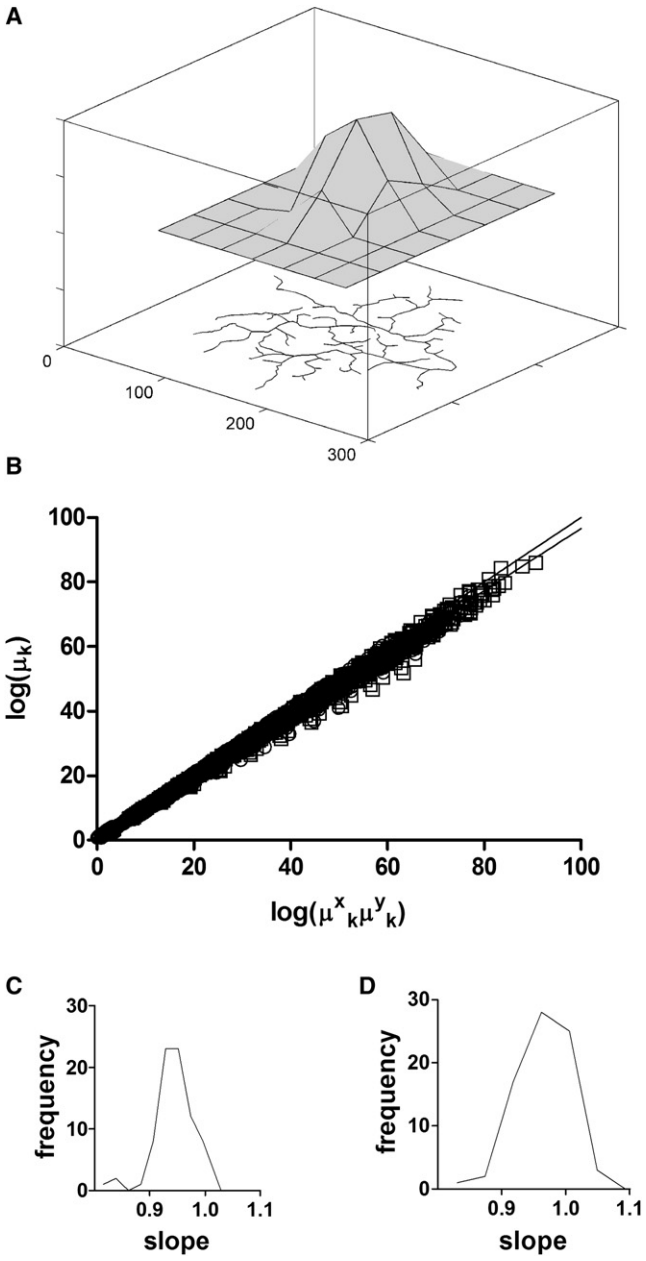

Figure 1. Separability Test for the Two-Dimensional Dendritic and Axonal Arbors

Data from goldfish and zebrafish retinotectal axonal arbors (n = 79) and retinal ganglion cell dendritic arbors (n = 76).

(A) An arbor density function estimated by summing the arbor's segment lengths in each box of a grid (6 × 6) covering a goldfish retinotectal arbor shown beneath the estimated density. Length indicated on axis in microns.

(B) Double logarithmic plot of the product moment (m_k, $k = 0,2…20$) as a function of the product of the separated moments ($m^x_k m^y_k$). Squares are for axonal arbors, and circles (obscured by the density of data points) are dendritic arbors. The equality line (top, slope = 1) and a least-squares line fitted to all 1705 data points from 155 arbors (slope = 0.966 ± 0.001) can be seen extending past the cloud of data points.

(C) Frequency histogram of slope for $\log(m_k)$ versus $\log(m^x_k m^y_k)$, calculated by least-squares, for each of the 79 retinotectal arbors.

(D) Frequency histogram as in (C) for 76 retinal ganglion cell dendritic arbors.

function (so that averaging them is justified) or how to align, and possibly scale, the arbor densities from different arbors.

Our goal, then, is to find a way of characterizing the arbor density for individual arbors without making assumptions about the density function's form. Initially, we will restrict our attention to two-dimensional arbors from goldfish and zebrafish visual systems (retinal ganglion cell dendritic arbors and retinotectal axonal arbors), like the one illustrated in Figure 1A, and then consider mammalian three-dimensional arbors.

The problem with working directly with arbor densities is that density is a local property of an arbor (each point in space is assigned a value of the density) and therefore is noisy. To describe individual arbors with good resolution and without making assumptions about their form, we need a way of transforming the arbor's density function in terms of less noisy global parameters (each one of which reflects information about the entire arbor) rather than local parameters. To do this, we have borrowed a standard method from probability theory in which a probability distribution is completely characterized not by its density but rather by its moments, like the mean, standard deviation, kurtosis, and higher moments. Knowing all of the moments of a probability distribution is exactly equivalent to knowing the function that describes that distribution, but moments are global parameters; the value of each moment depends on the entire arbor.

We have used this same moment approach to characterize arbor density functions. Arbor moments (defined below) are easy to calculate, and the number of moments calculated determines the resolution with which the density function is described. Generally, when the number of moments is doubled, the resolution also doubles, and we have used 21 moments to give a resolution of about 1/20th of the arbor's diameter. The lower-order moments characterize the arbor density function, and information about the fine details of arbor structure (exact location and shape of individual branches) only begins to appear when a very large number of moments have been calculated (Stevens, 1982).

We seek simplicities underlying arbor structure and, thus, start by identifying ways that arbors could be constructed to make the density function as simple as possible. Two requirements for the greatest possible simplicity are immediately apparent. The first requirement is that it should be possible to change the arbor's distribution along one direction without affecting the shape of the arbor's density in other orthogonal directions. In this way, changing the density function in each direction would not influence the density function in other directions. The second requirement is that only one—or perhaps a few—different functional forms should be used to specify arbor density functions. If arbors differed from one another only by being stretched or shrunken along major orthogonal axes, then rules that determined connections between arbors during development would have to take account of just a few parameters per arbor. These parameters, together, of course, with the propensity of the two particular cell types to synapse, could then specify the probability of two arbors coming close enough and forming a synapse.

Both of these requirements relate to qualitative properties of arbor density functions. The first property is *separability* (arbor densities in the *x* and *y* directions are independent), and the

second is known as *self-similarity* (arbor densities have the same shape, up to some stretching or compression). There are no standard tests for these properties, so we have developed ones to discover whether arbor density functions are separable and self-similar and also to determine how many different functional forms for density functions are used by the brain. These tests can be carried out by plotting the measured arbor moments in ways described below. The goal of the following sections is to show that the arbors we have examined "pass" both of these tests: all arbors are nearly separable (we shall describe how close they come to exact separability) and can be described by a density function with a single functional form, a truncated two- or three-dimensional Gaussian. Thus, arbor densities are, we shall conclude, about as simple as they could possibly be.

Arbor Moments

All of the arbors we used were digitized using Neurolucida and thus are represented as a collection of very short line segments, with the i^{th} segment having, for the two-dimensional arbors, a midpoint location (x_i, y_i). The moments we calculate are all weighted averages of these segment midpoint locations raised to some power; the weight assigned to each segment in this average is its length. For reasons that will become clear later, we use two sorts of moments, described first for two-dimensional arbors. The first kind of moments are called here "product moments," denoted by m_k. To calculate m_k, we sum oven all segments the quantities $(x_i y_i)^k$—the product of the i^{th} segment midpoints $x_i y_i$ raised to the k^{th} power—with the i^{th} quantity weighted by i^{th} segment length. The integer k is called the *moment order* and ranges from 0 to 20 in the following. For what is designated "separated moments," we sum over all segments in the arbor (again with the weight being determined by the arbor length for each segment) either $x^k{}_i$ or $y^k{}_i$, the x or y segment midpoint coordinates raised to the k^{th} power. These separated moments are denoted $m^x{}_k$ or $m^y{}_k$. Note that the x and y here are superscripts indicating whether x_i or y_i was averaged, and are not powers. The moments are defined in the same way for the three-dimensional arbors, except that the three coordinates (x_i, y_i, and z_i) are needed to give the location of the midpoint of each segment. In Experimental Procedures (Calculation of Arbor Moments), we give a more detailed description of how moments are calculated.

Arbor Density Separability (2D Arbors)

We start by asking whether arbor density functions are separable in Cartesian (x,y) coordinates. Any function $f(x,y)$ is separable if it can be written as the product of two functions $g(x)$ and $h(y)$: $f(x,y) = g(x)h(y)$. What this means is that the function $f(x,y)$ can be changed in the y direction, by stretching $h(y)$, for example, without altering the function $g(x)$ in the x direction. For example, the function

$$f(x,y) = e^{-(x^2/a^2 + y^2/b^2)} = \left(e^{-x^2/a^2}\right)\left(e^{-y^2/b^2}\right)$$

is separable because it can be written as a product of the two functions indicated above, and stretching the function in the y direction (by changing b) has no effect on its x dependence. An example of a function that is not separable is $f(x,y) = \exp(-(xy)^2)$, where $f(x,y)$ would extend a larger amount over space in the x direction than $f(x,2y)$.

If an arbor's density is separable, then the product moments defined above equal the product of the separated moments (see Experimental Procedures: Theory), for moments of all orders: $m_k = m^x{}_k m^y{}_k$, for all k. Because the moments m_k become very large (m_{20} is close to 10^{80} for the largest fish arbors), we plot $\log(m_k)$ against $\log(m^x{}_k m^y{}_k)$ for $k = 0,2\ldots20$ in Figure 1B. If the densities for fish retinal ganglion cell dendritic and axonal arbors are separable, they should fall along the equality line with a slope of 1 that passes through the origin. Clearly, the arbor density functions tested in Figure 1B for both the dendritic and axonal arbors are approximately, but not exactly, separable: although the line fitted to the data passes through the origin, the slope of $\log(m_k)$ against $\log(m^x{}_k m^y{}_k)$ is a few per cent less than 1. The deviation from exact separability is documented in Figures 1C and 1D, where histograms for all slopes of $\log(m_k)$ versus $\log(m^x{}_k m^y{}_k)$ for individual arbors appear. Exact separability (with some random error) should have slopes distributed around 1, but the observed slopes are distributed around 0.95 for dendritic arbors (Figure 1C) and 0.97 for axonal arbors (Figure 1D).

Clearly, these arbor density functions are "almost" separable, but how are we to interpret the observed departure from exact separability. Although there is no standard way for quantitating how close a function comes to being separable, there is in this case a natural way to measure departures from exact separability. The only two-dimensional function that is circularly symmetric and separable in Cartesian coordinates is a Gaussian (Jaynes, 2003), but a Gaussian truncated at a circular boundary (a Gaussian-like function that vanishes outside of the circular boundary) would no longer be separable (see Suplemental Experimental Procedures: Arobr Separability). As the location of the truncation moves farther from the center (measured in number of standard deviations to the truncation boundary), the departures from exact separability decrease smoothly until, when the truncation moves to infinity, the function is exactly separable. Deviations from exact separability, then, can be measured in terms of the distance in standard deviations to the boundary where the Gaussian's value vanishes.

Because many of the fish arbors are approximately circular, close to separable, and terminate at their boundaries, a truncated Gaussian arbor density function should be a reasonable description, and the deviation from separability can be specified as the location of the arbor territory boundary measured as number of standard deviations. Using the equations derived in Suplemental Experimental Procedures: Arbor Separability, we have evaluated the data presented in Figure 1B and find the departure from exact separability is what would be expected if the arbors were, on average, described by a Gaussian density function that was truncated at about two standard deviations. Figure S1 documents the departure from separability with a related but different method with the same conclusion.

Our use of a truncated Gaussian to quantitate the departure from exact separability certainly does not mean that the arbor density function must be a truncated Gaussian, but it does reveal how deviations from exact separability of the magnitude found

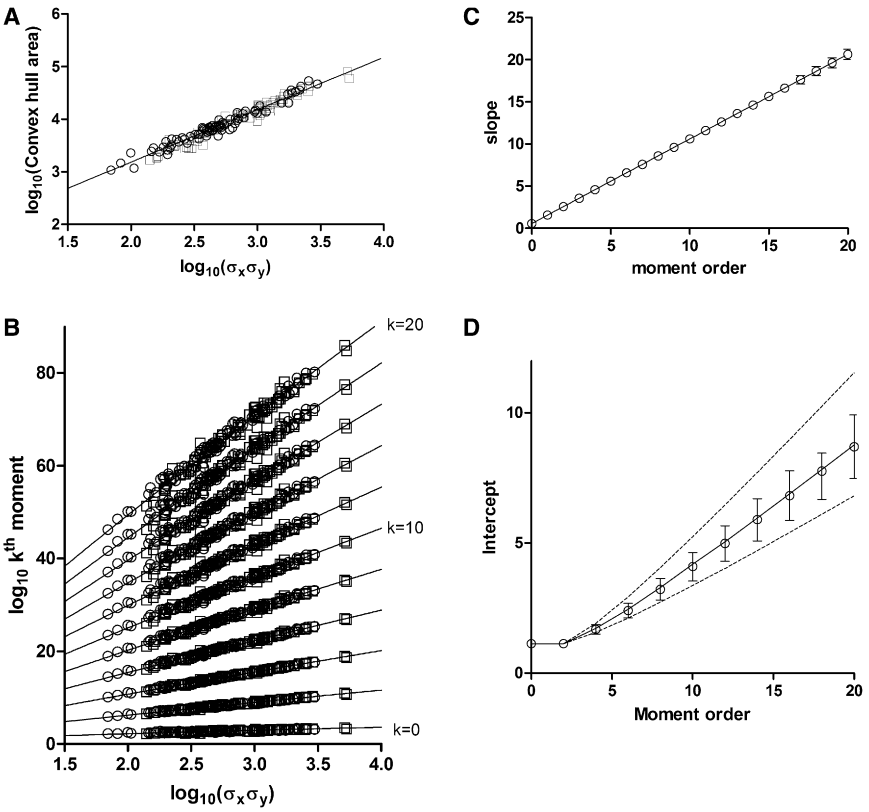

Figure 2. Properties of the Arbor Density Function of Two-Dimensional Axonal and Dendritic Arbors

(A) Double logarithmic plot comparing of the size of arbors measured by their convex hull area (units: μm^2), with arbor size measured by the product of the arbor standard deviations in the x and y directions (units: μm^2). Squares represent data from 79 axonal arbors and circles from 76 dendritic arbors. Least-squares line has a slope = 1.013 ± 0.017 and intercept 1.135 ± 0.047.

(B) Plot of log(m_k) as a function of log(σ_x σ_y) for $k = 0,2…20$. Circles for dendritic arbors and squares for axonal arbors. Each arbor provides a single point for each k for a total of 1705 data points on the graph. Straight lines superimposed on data points are from least-squares fits.

(C) Slopes of least-squares fits to log(m_k) as a function of log(σ_x σ_y) for moment orders (k) with $k = 0,1…20$. 95% confidence intervals are just visible for the last four data points; for other data points, the 95% confidence intervals are smaller that the radius of the plotting symbols. The straight line superimposed on data points has a slope of 1.005 ± 0.0001 and an intercept of 0.546 ± 0.002 determined by a least-squares fit.

(D) Intercepts of regression lines in (B) as a function of moment order. Error bars are 95% confidence intervals. The smooth curve through the points is what would be predicted from a Gaussian arbor density function truncated at a circular boundary at 1.95 standard deviations from the center of the arbor. The upper smooth line is the prediction of a Gaussian truncated at a circular boundary at 2.95 standard deviations, and the lower smooth line is the prediction of an arbor density function, normalized to have the observed arbor standard deviation, with a constant density inside a circular boundary.

could naturally arise and gives a feeling for the magnitude of the effect. In summary, then, we can say that arbor density functions for the Figure 2 data are nearly separable, so an arbor's density could be stretched or compressed (or modified in other ways) in one direction without appreciable changes in an orthogonal direction.

Measures of Arbor Size (2D Arbors)

Arbors vary greatly in size from one neuron to the next, and we wish now to compare the density functions, as reflected in their moments, for arbors with different sizes of territories. We need, then, to identify a quantitative measure of territory size. A first possible measure, one often used to specify the size of retinal ganglion cell dendritic arbors (Wässle and Boycott, 1991), is the area of the smallest enclosing convex polygon (the convex hull). A second potential size measure is the product of the standard deviation of the arbor in the x and y directions, which is

$$\sigma_x\sigma_y = \sqrt{\frac{m_2^x m_2^y}{m_0}};$$

the arbor length m_0 appears here to normalize the total arbor "weight" to 1 so arbors with different lengths can be compared. Figure 2A presents a double logarithmic plot of convex hull area as a function of $\sigma_x\sigma_y$ for our fish arbors, and the superimposed line is a least-squares fit to the data with a slope of 1.013 and an intercept 1.135 = log(13.6); thus, the quantity $\sigma_x\sigma_y$ is proportional to the territory area (estimated by the convex hull) so that these two measures of arbor size are equivalent. We use $\sigma_x\sigma_y$ as our measure of territory size in the following. This size measure was selected to provide a simple test for self-similarity described in the next section.

Because the convex hull area A of arbors is proportional to the product $\sigma_x\sigma_y$ with $A = \pi r^2 = 13.6\sigma_x\sigma_y$, ($r$ is the equivalent radius that gives a circle of area A, and the 13.6 comes from the intercept of the regression line in Figure 2A), the distance r to the arbor boundary can be expressed in units of the average standard deviation $\sigma = (\sigma_x\sigma_y)^{1/2}$. For the fish retinal ganglion cell dendritic arbors and retinotectal axonal arbors, $r = 2.08\sigma$, a value similar to what is needed to account for the deviation in Figure 1B from exact separability.

Arbor Density Self-Similarity (2D Arbors)

In the preceding, we have shown that arbors are characterized by density functions that are very nearly separable and have established a measure of arbor territory size ($\sigma_x\sigma_y$). We now turn to the question: what functional forms do arbor density functions have? We do not know in advance how many different functional forms the brain might use for arbors. We define a *class* of arbors as all arbors characterized by a density function with a single functional form. For example, all of the arbors that could be described by a Gaussian density function would

constitute one class, and arbors described by a pill-box function (constant arbor density inside a circular boundary, zero outside the boundary) would define a second class of arbors. A third class of arbors might be described by a doughnut-like density function.

Earlier, we pointed out that, in addition to separability, another desirable property for a density function is that it have the same shape for all arbors in the same class, but the arbor density is perhaps stretched or compressed from one arbor to the next within the class. For example, a class of arbors might be described by pill-box functions, but members of this class might have pill-boxes with different diameters. And some members of the class might be described by pill-boxes with an elliptical shape where the diameter in one direction would be stretched more than the diameter in the orthogonal direction. Functions that have the same shape (for example, pill-box) but differ only in being smoothly stretched or compressed along one or more orthogonal axes (circular and elliptical pill-boxes of different sizes, for instance) have been studied, and are called *self-similar functions* (Barrenblatt, 1996; also see Supplemental Experimental Procedures: Self-Similar Functions for a more complete description of this class of functions and for examples of families that are and are not self-similar).

To determine the extent to which an arbor density function is, indeed, self-similar, we have developed a test using the arbor moments m_k that appeared above in our study of separability. In this test, the moments for all arbors from one class fall along one set of lines, and the moments for arbors of another class will fall along a second set of lines. Thus, the test determines how many classes of arbors are present and whether the arbors of each class have the property of self-similarity (all density functions have the same shape, except for being stretched or compressed in one or more directions).

This test for self-similarity for arbors in the same class (see Experimental Procedures: Theory) takes place in two steps. The first step is to plot, for different arbors, $\log(m_k)$ versus $\log(\sigma_x\sigma_y)$ for the various values of $k = 0,1,\ldots.20$. Arbors that share a self-similar density function should fall on straight lines, with a different slope for each value of k. The second step in the test is to plot the slope of each line generated in the first step versus the associated value of k; if the function is self-similar, the slope of this plot should be 1 with an intercept that is not known in advance. Note that in this test for self-similarity, every individual arbor is compared to all other arbors because each arbor is represented by its 21 quantities, the values of its 21 moments, that appear in our plots. Any specific arbors that deviate systematically from others can be identified by visual inspection.

This test can fail for two reasons. The first reason is that the density function that describes the arbors being tested is not a self-similar function. The second reason is that arbors of different classes, that is, with different functional forms for their density functions, are being compared. This second type of failure can occur even if each of the different classes into which the arbors fall is described by a self-similar density function. When data from multiple classes of arbors are superimposed, the data points do not, as described below, fall on a single set of lines, and the result can be difficult to interpret. In general, it might be hard to identify the cause for a failure of the self-similarity test, but if the test is "passed," this must mean that the arbors being compared are all described by a density function with a single functional form (all fall into the same class).

The test for self-similarity as just described gives no information at all about the shape of the density function being studied, and a function of any shape at all that is altered by smoothly stretching or compressing along orthogonal axes will pass the test. All of the information about the shape of the density function is contained in the intercepts of the lines fitted in the first step of the test for self-similarity. Different functions each have a different pattern of intercepts as the moment order varies, and any proposed density function can be tested to see whether it provides an adequate description of the data by comparing the observed and predicted pattern of intercepts (see Experimental Procedures: Intercepts for self-similarity test). Going from the moments of a function to the function itself is, however, an old problem that is unsolvable without additional constraints (Jimbo, 2004). The more similar in shape two functions are, the closer their pattern of intercepts, so one can say, as will be seen, that whenever the moments of density functions for different arbors fall close to the same set of lines, those arbors must have density functions that are nearly the same shape.

Figure 2B is a plot, for $k = 0,2,\ldots20$ (see Figure S4 for a plot of all 21 moments), of $\log(m_k)$ versus $\log(\sigma_x\sigma_y)$ (first step in test for self-similarity) for the 155 fish retinal ganglion cell dendritic arbors and retinotectal axonal arbors that provided the data for Figures 1 and 2A. These data do not differ significantly from a single set of straight lines (fitted by least-squares) as required to pass the first part of the test for a single self-similar density function. Figure 2C is a plot of the slope of each line for $k = 0,1,\ldots20$ in Figure 2B (and for odd-numbered moments not shown in Figure 2B; see Figure S4) as a function of the corresponding moment order k (second step). The slope of the line in Figure 2C, predicted to be 1, is determined by a least-squares fitting of the data to be 1.005 and is not significantly different from 1. Clearly, our population of fish arbors can all be described by a single density function that is self-similar.

The results from Figure 2 we have discussed above mean that, because the data in Figure 2B are well fitted by a single set of lines, the same self-similar arbor density function describes all of the fish dendritic and axonal arbors we have examined. But the data as presented do not uniquely specify the functional form of the density function. As noted above, any self-similar function will pass the test we have used, but different self-similar functions will have different patterns of intercepts for the various arbor moments. As an example, Figure 2D shows the measured intercepts from Figure 2B and the predictions (see Experimental Procedures: Intercepts for self-similarity test) from a Gaussian density function truncated at 1.95 standard deviations at a circular boundary (line passing through the data points). Predictions from the closely related Gaussian density function truncated at 2.95 (upper theoretical line) show that this relatively small change in the density function (truncating the Gaussian at one additional standard deviation) is clearly a poor fit. Another possible density function is a "pill-box," a density function that assumes uniform coverage by the arbor within its boundary, but it is also unsatisfactory (lower theoretical line). We can say,

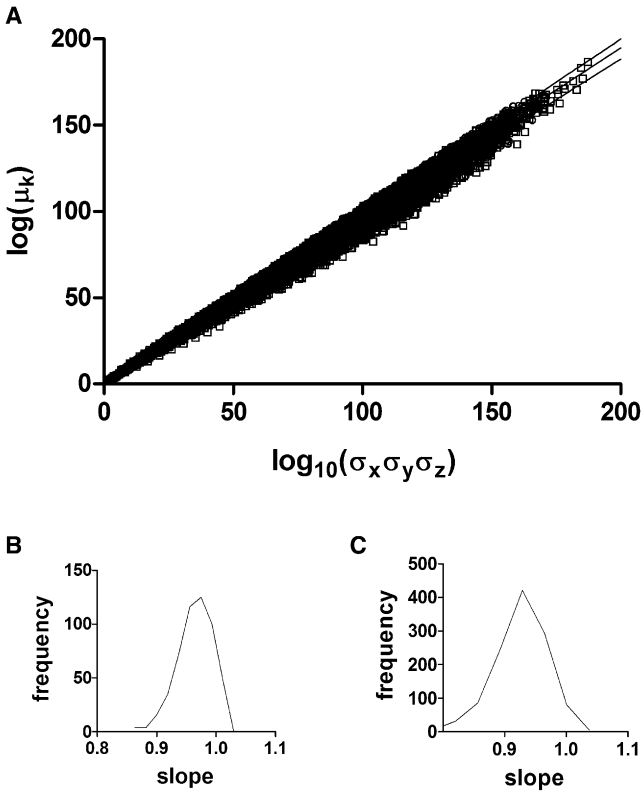

Figure 3. Separability Test for Three-Dimensional Axonal and Dendritic Arbors from Mammalian Neurons

(A) Double logarithmic plot of the product moments (m_k) as a function of the product of separated moments ($m^x_k m^y_k m^z_k$) for $k = 0,2,\ldots20$. The plot is based on data from 1091 neocortical axonal and dendritic arbors (squares) and 521 hippocampal arbors (both axonal and dendritic plot symbols are obscured because the graph contains 18,590 data points). Three straight lines have been fitted to the data and can be seen extending from the cloud of data points. The upper line has a slope = 1. A regression line, fitted to the data from hippocampal cells and constrained to pass through the origin, has a slope of 0.975 ± 0.0004 and appears in the middle. The lowest regression line, with a slope of 0.942 ± .0003, was fitted to the neocortical data points.

(B) Frequency histogram of slopes fitted to log(m_k) as a function of log($m^x_k m^y_k m^z_k$) for 521 individual hippocampal arbors with $k = 0,2\ldots20$.

(C) Frequency histogram, as in (B), from 1091 neocortical arbors.

then, that if we approximate the fish arbor density function as a Gaussian truncated at 1.95 standard deviations, we have a statistically adequate and very compact description for all of the data in Figures 1B and 2B–2D. Although we can exclude a Gaussian that is truncated at 2.95 standard deviations, and a pill-box density function, there is a range of functions close to a Gaussian truncated at 1.95 standard deviations that we cannot exclude.

Nevertheless, we have achieved a simple and statistically adequate description of the data in Figures 1B and 2. The 1705 data points in Figure 2B (and 3255 data points in Figure S4) can be predicted (neglecting scatter) with just two numbers: the intercept of the straight line in Figure 2C (0.546) and the location of the arbor truncation (1.95 standard deviations) for a Gaussian density function.

Three-Dimensional Mammalian Arbor Densities

Does the simplicity of the arbor density function found for the two-dimensional fish arbors described above extend to three-dimensional arbors in the mammalian brain? We have tested the density functions of 1612 arbors from the mammalian brain for separability and self-similarity. These arbors were reconstructed in Neurolucida, and include axons and dendrites from various neocortical areas in humans, monkeys, cats, and rodents (1091 arbors) and from the rat hippocampus (521). Pyramidal, stellate, granule, and a wide variety of inhibitory cell types—reconstructed by 22 different laboratories—are included (see Experimental Procedures). For pyramidal cells, we calculated the moments for basal and apical dendritic arbors separately. Although not an issue for the reconstructions that we have used, we would have excluded long, unbranched segments as part of an arbor. For example, if an axon arborized in two well-separated locations, we would consider this as two different arbors and exclude the connecting, unbranched axon connecting the two arbors.

Figure 3A (the separability test) displays a double logarithmic plot of the product moment m_k as a function of the product of the separated moments $m^x_k m^y_k m^z_k$, for even values of $k = 0$ to 20. As with the two-dimensional fish arbors, these three-dimensional arbors fall close to the equality line but depart from exact separability. The slopes of log(m_k) versus log($m^x_k m^y_k m^z_k$), determined by a least-squares fit for individual arbors, appear in the histograms for neocortex (Figure 3B) and hippocampus (Figure 3C) with $k = 0,2,\ldots20$. As for the fish arbors, the magnitude of these deviations from exact separability is what would be expected for a three-dimensional Gaussian density function truncated at around two standard deviations (also see Figure S2, which documents departures from exact separability in a related but different plot).

We also carried out the two-step test for self-similarity of the arbor density functions. For the first step of the test, Figure 4A displays a double logarithmic plot of the product moments m_k as a function of arbor size as measured by the product $\sigma_x\sigma_y\sigma_z$ together with least-squares fits to the data for moments $0,2,\ldots20$ (see Figure S6 for all moments). As with the fish arbors, the data fall along a single set of straight lines for moment values that range over about 175 orders of magnitude (up to 10^{175}). In the second step of the test for a single self-similar density function, the slopes of the fitted lines in Figure 4A (together with the slopes fitted to the odd-numbered moments not presented in the figure; see Figure S5) are plotted as a function of the moment order k in Figure 4B. The least-squares fit to the data in Figure 4B, predicted to have a slope = 1, has a slope of 1.035. As with the fish arbors, then, these mammalian arbors all share (within the statistical limits of our resolution) a single self-similar density function, because data points fall along a single set of lines, one for each moment order.

Finally, the intercepts for the least-squares fits to the Figure 4B data are plotted as a function of moment order (k) in Figure 4C. Superimposed on these observed intercepts are those expected if the arbor density function were a three-dimensional spherical Gaussian truncated at 1.7 standard deviations (curve through the data points). For comparison, the predicted intercepts for a Gaussian density function truncated at 2.7 standard deviations

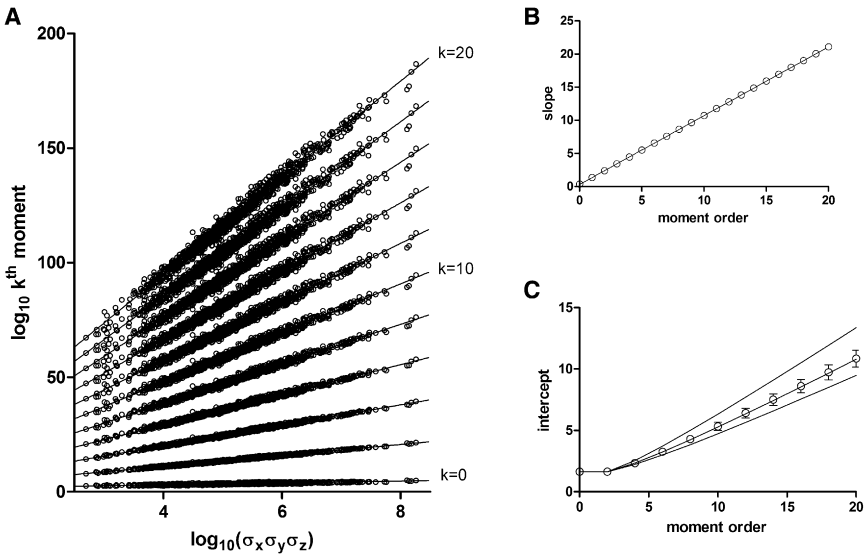

Figure 4. Test for Self-Similarity of Three-Dimensional Mammalian Arbors

(A) Double logarithmic plot of m_k as a function of $\sigma_x\,\sigma_y\,\sigma_z$ for 1091 neocortical and 521 hippocampal arbors (both axonal and dendritic) for $k = 0,2\ldots20$. Each of the 1612 arbors provided a data point for each k. Straight lines are least-squares fits, one for each value of k.

(B) Plots of slopes of regression lines fitted to $\log(m_k)$ as a function of $\log(\sigma_x\,\sigma_y\,\sigma_z)$ for the arbors represented in (A) with $k = 0,1,2,\ldots.20$. 95% confidence intervals for each slope is less than the radius of the plot symbol. The regression line plotted over the data points has a slope = 1.035 ± 0.001 and an intercept = 0.332 ± 0.011.

(C) Intercepts of the regression lines that appear in (A) as a function of moment order. The error bars indicate 95% confidence intervals. The line through the data points is predicted from a Gaussian arbor density function that is truncated at 1.7 standard deviations. For comparison, the predictions of a Gaussian arbor density function truncated at 2.7 standard deviations (top smooth line) and an arbor density function (normalized to have the observed intercept for $k = 2$) with constant density inside a spherical boundary.

(upper theoretical curve) and a three-dimensional pill-box density function that has constant density within the arbor boundaries (lower theoretical curve) are displayed (see Experimental Procedures: Intercepts for self-similarity test) and are outside the 95% confidence limits. We can say, then, that a truncated Gaussian gives, in a statistical sense, a satisfactory description of our population of three-dimensional mammalian arbors. The 17,831 data points in Figure 4A (and 33,852 data points in Figure S5) are described (neglecting scatter) by just two numbers: the intercept of the line in Figure 1B (0.332) and the location of the truncation of the Gaussian fitted to the data (1.7 standard deviations).

DISCUSSION

We have shown that the density functions for all of the arbors we have examined share two qualitative properties: the density functions are very close to being self-similar and separable. When we started our analysis, we had anticipated that arbors would fall into a number, possibly a large number, of distinct classes, each characterized by its own functional form for its arbor density function. But—within the limits of our resolution—we find that all arbors can be described by a single density function. On reflection, this observation is perhaps less surprising than we first thought. Because the genetic networks responsible for pattern formation are frequently conserved through evolution, comparable structures with different sizes often are described by self-similar functions (Stevens, 2009), and one might anticipate that a single set of pattern formation rules could be used to generate most or all arbors.

How sensitive is the test we have used for self-similar functions? That is, how firm is our conclusion that the arbor density function is, indeed, self-similar and to what extent can we confidently conclude that all arbors are described by the same functional form? It is a remarkable fact that the functions describing the smooth stretching and shrinking of the arbors must, if the arbor density function is self-similar, be power functions (see Stevens, 2009, for a proof and references). This is the origin for the requirement that the lines in Figures 2B and 4A are straight rather that being curved, and there are many examples of functions for which curved lines occur in these plots (see, for example, Supplemental Experimental Procedures: Self-similar functions for families of functions that would not pass our test for self-similarity). This is also the source of the requirement that the plots in Figures 2C and 4B have a slope of 1 and, again, the first test for self-similarity might be passed and the second not. In both cases, the predictions made by the requirements of self-similarity are not, in the statistical sense, significantly different from the data. What we can say, then, is that, within the scatter of the data, all arbors can be described by a single self-similar arbor density function. We do not know what fraction of the scatter observed in our plots is the result of noise in estimating density function moments from sparse arbors and what fraction might arise from small departures from self-similarity or the presence of very similar multiple functional forms for the arbor density functions.

We can also conclude that all of our data can be adequately described—in the sense that predictions based on a truncated Gaussian are not statistically different from the data—by a density function that is a truncated Gaussian. Figures 2D and 4C demonstrate that the properly truncated Gaussian gives a good fit and that two alternative candidate density functions—a Gaussian truncated at one additional standard deviation and a uniform density—can clearly be excluded. Obviously, though, a range of potential arbor density functions cannot be excluded, those that are close enough to the best-fitting truncated Gaussian to fall within our window of uncertainty.

Our final conclusion is that arbor structure is governed by a simple general principle (all arbors are described by a truncated

Gaussian density function), but often general principles have exceptions. Are there arbors whose density function cannot be described by a truncated Gaussian? We have not examined invertebrate arbors, but we expect that some, perhaps many, may depart from the description given above. For vertebrates, one obvious nonconforming case is the class of arbors formed by cerebellar parallel fiber axons that must fit a one-dimensional pill-box density function. Another potential case that comes at once to mind is the class of two-dimensional mammalian arbors like the dendritic trees of cerebellar Purkinje cells and hippocampal neurons grown in cell culture. The databases available unfortunately have only a small number of mammalian two-dimensional arbors. Those arbors that are available, however, appear to have the same density function as the fish arbors, because their moments fall along the least-squares lines fitted to fish axonal and dendritic arbors in Figure 2B (see Figure S6 for Purkinje cell dendritic arbors and hippocampal neuron dendritic arbors grown in cell culture). Because the sample size is small, we feel that no definite conclusions can be drawn about the available mammalian two-dimensional arbors, but we have no evidence that these arbors differ from the two-dimensional fish arbors.

The simple design principle for arbor structure we have discovered immediately leads to two classes of questions. How is this principle implemented during the development of arbors? And why did evolution select this particular principle?

Arbors seem to grow by extending trial branches that are either stabilized by synapse formation or withdrawn (Cline, 2001; Niell and Smith, 2005). Furthermore, the branches of an arbor avoid one another and do not touch (Gao, 2007). Such a process can be described as a self-avoiding random walk, and it is therefore surprising that a Gaussian density function results. It is well known that a random walk will generate a Gaussian density function, but it is also well known that self-avoiding random walks result in non-Gaussian density functions (de Gennes, 1979). This means that there must be some special feature of arbor growth that distinguishes it from the self-avoiding random walks that have been studied. When this feature is identified, an important biological question will also have been identified: what is the molecular biological basis for those particular arbor growth rules that are responsible for generating Gaussian arbor density functions.

The question of why evolution selected the Gaussian arbor density function can be answered in different ways. One way is to consider the computational advantages of a Gaussian density function, and a second way relates to the development of neural circuits.

The Gaussian is a unique function with properties that should be advantageous for arbors whose job is to distribute and sample information displayed in neural maps. One of the special properties of Gaussians, their separability, has been discussed above. A second unique property is that the Gaussian is the function of a given size (measured by the standard deviation) that has the maximum entropy. What this means is that a Gaussian arbor distributes or samples information in the most random way over its territory so that synaptic partners will have the best chance of finding their correct mate and arbor "traffic jams" would be minimized. A recent study of pyramidal cell basal dendrites (Wen et al., 2009) also used a statistical approach to describe arbors and found that the same spatial correlation function could fit the data from many of the arbors in their sample. These workers also argued that the arbor structure maximizes entropy for a given arbor length and territory size (related to our second product moment).

Although our understanding of axon guidance, map formation, and neuronal fate determination has grown rapidly in recent years (Bertrand et al., 2002; Charron and Tessier-Lavigne, 2007; Clandinin and Feldheim, 2009; Flanagan and Vanderhaeghen, 1998; Hsieh and Gage, 2004; Jessell, 2000; Louvi and Artavanis-Tsakonas, 2006; Luo and Flanagan, 2007; Price et al., 2006; Tessier-Lavigne and Goodman, 1996), we still know little about how synaptic partners are selected, a crucial step in the formation of neural circuits. One popular theoretical possibility is that each synaptic connect is uniquely specified. Another possibility is that connections are made at random with a probability that is related to the chances that pre- and postsynaptic partners happen to find each other and the probability that the particular partners will form a synapse depending on the cell types involved. The first alternative involves, as noted in the Introduction, the use of a vast quantity of information, whereas the second possibility seems, given what is known about map formation (Clandinin and Feldheim, 2009; Luo and Flanagan, 2007; Price et al., 2006), to be a more easily believable alternative for the vertebrate brain.

The simplicity of arbor form that we have discovered makes the second possibility even easier to implement and could be the reason evolution has selected this simple design principle for arbor structure. The economy of a single density function for all arbors means that any arbor can be described by just a few parameters: location in the brain of the arbor's center of mass (three parameters), orientation in the brain (two parameters), and a dilation factor in three orthogonal directions (three parameters). This minimal characterization of arbors suggests a rather simple model for circuit development. Neurons have an identity that depends on their location and time and place of birth, and each neuron needs to know where to put its arbors, what orientation the arbor should have, and how far it is to grow in each of three directions. Synapses are then made in a way that depends on the probability that one arbor (an axon, for example) will be able to contact another arbor (a dendrite)—this probability depends jointly on the arbor density functions—and on the probability that one cell type will make or accept a synapse with another cell type. Such a view is very simple, and the most difficult part is how one cell decides to synapse with another, something that is poorly understood.

An even simpler mechanism can be envisioned. One might suppose that a cell uses spatial cues to decide where its arbor should reside and then makes synapses with acceptable targets in that region until the number of targets has been exhausted. This type of model could perhaps, with the proper rules, generate the arbors with the properties we describe and account for how circuits are formed.

EXPERIMENTAL PROCEDURES

Arbor Visualization

Goldfish (*Carassius auratus*) were obtained from local pet stores and zebrafish (*Danio rerio*) were maintained in the Salk Institute animal facility. Fish were anesthetized with 0.1% tricane methanesulfonate and perfused through an intracardiac catheter constructed from a glass micropipette. For perfusion, phosphate-buffered saline (0.8 M PBS), followed by 4% paraformaldehyde

was used. For DiI (Molecular Probes, Eugene, OR) staining of retinotectal arbors, the brain was removed from the fish, fixed in 4% paraformaldehyde for 2 hr, and a small crystal of DiI was inserted into a nick in the optic nerve. The brain was maintained in fixative at 37°C for about 5 days and then whole-mounted in fixative and scanned with a confocal microscope (LSM510; Carl Zeiss, Thornwood, NY). Arbors in the confocal stack were reconstructed with Neurolucida (Microbrightfield, Williston, VT).

For Figures 1 and 2, we also used retinal ganglion cell dendritic arbors from zebrafish and goldfish of different sizes. These arbors have been described earlier (Lee and Stevens, 2007).

Arbors (Figures 3 and 4) from various neocortical areas and hippocampus and including various cell types and species (rat, cat, monkey, and human), reconstructed in Neurolucida by 22 laboratories, were downloaded from the database at Neuromorpho.org; we used all of the arbors available on June 13, 2007, for "cortex" (1091) and for "hippocampus" (521), except that hippocampal neurons grown in culture were excluded. The hippocampal arbors from cultured cells and cerebellar Purkinje cell dendritic arbors gave data for Figure S6. All of the mammalian neurons that we have studied can be viewed and additional information about them found at Neuromorpho.org.

Calculation of Arbor Moments

How are arbor moments calculated? Teleost (zebrafish and goldfish) retinal ganglion cell arbors, which we consider first, are flat, disk-like structures (Figure 1A) that can be reconstructed as a stick figure consisting of many straight, short segments; the center of the i^{th} segment is at location (x_i, y_i) and the length of this segment is w_i. The total length m_0 of the arbor is, for an arbor approximated by N segments, just the sum of the lengths of all of the segments; the 0^{th} moment (denoted as m_0) then is

$$m_0 = \sum_{i=1}^{N} w_i.$$

The $(j,k)^{th}$ moment $m_{j,k}$ is defined as

$$m_{j,k} = \sum_{i=1}^{N} x_i^j y_i^k w_i.$$

Although moments are defined for any pair of positive integers j and k, in practice we will need only ones for which $j = k$ or either j or k is zero. If $j = k$, so both coordinate variables are raised to the same power, we use the shorthand notation $m_k = m_{k,k}$ (note the single subscript) and call this a product moment. When the exponent for either x or y is zero, we use the notation

$$m_k^y = m_{0,k}/\sqrt{m_0} \text{ or}$$

$$m_k^x = m_{k,0}/\sqrt{m_0}$$

and refer to these as the separated moments in the y or x direction. The quantity

$$\sqrt{m_0}$$

appears in the definition of the separated moments because the weights w_i are not normalized to sum to 1 (like a probability) but rather sum to the total arbor length m_0; this normalization is required later for the test of separability that follows. Later we shall consider three-dimensional arbors. For these arbors, the moments involve the product (x_i,y_i,z_i), and we have, in addition, the separated moment m^z_k. Furthermore, the separated moments for the three-dimensional arbors are normalized by $m_0^{2/3}$ rather than by $m_0^{1/2}$ as are the separated moments for the two-dimensional arbors.

Because the densities of the many arbors are nearly circularly symmetric (spherically symmetric for three-dimensional arbors), the odd-numbered moments vanish on average. To still make use of the information contained in the odd-numbered moments for all arbors, we calculate product moments as

$$m_{j,k,l} = \sum_i |x_i^j y_i^k z_i^l| w_i,$$

with $l = 0$ for the two-dimensional arbors, except (see next paragraph) for the product moment m_1 and the separated moments $m^x{}_1$ and $m^y{}_1$ where the absolute value is not used.

We take the arbor's center of mass as the origin of the coordinate system so that $m^x{}_1 = m^y{}_1 = 0$, rotate the arbor so that the arbor's covariance $m_{1,1} = \Sigma_i(x_i y_i)w_i = 0$ (or $m_{1,1,1} = 0$ and $m^z{}_1 = 0$ for three-dimensional arbors), and calculate the first 21 moments (0 through 20) for each arbor.

Theory

The definition of a self-similar function $f(x.\lambda)$ is, for present purposes, that the function conforms to the relation $f(x,\lambda) = \lambda^h f(x/\lambda,1)$ for every nonnegative size parameter λ and a fixed value of h (Barrenblatt, 1996). Here $f(x,\lambda)$ and its higher-dimensional versions with arguments (x,y) or (x,y,z) represent the arbor density function. If the arbor density depends on more than a single independent variable, then there may be a different size parameter for each dimension. For example, for two dimensions, a self-similar arbor density $f(x,y,\lambda_x,\lambda_y)$, with size parameters λ_x and λ_y for the x and y spatial variables, would have the property $f(x,y,\lambda_x,\lambda_y) = (\lambda_x\lambda_y)^h f(x/\lambda_x,y/\lambda_y,1,1)$.

For simplicity, some calculations below are carried out for a single dimension, and any differences in applying the equations to two- and three-dimensional arbors will be noted.

For a two-dimensional arbor density (assumed for simplicity to have a single size parameter λ), we use the product moment $m_k(\lambda)$ that is

$$\begin{aligned} m_k(\lambda) &= \int_{-\infty}^{\infty}\int_{-\infty}^{\infty} dxdy\left|xy\right|^k f(x,y,\lambda) \\ &= \int_{-\infty}^{\infty} dx\left|x\right|^k g(x,\lambda)\int_{-\infty}^{\infty} dy\left|y\right|^k g(y,\lambda) \\ &= m_k^x(\lambda)m_k^y(\lambda). \end{aligned}$$

The second step assumed that $f(x,y,\lambda)\ m_0(\lambda) = g(x,\lambda)g(y,\lambda)$ is separable and circularly symmetric, and the third step made use of the definition of the separated moments $m^x{}_k$ and $m^y{}_k$ that are defined by the integrals in the product just preceding. The relation above forms the basis for our separability test.

In order to use the arbor moments to test for self-similarity of the arbor density function, we must derive a relationship between various orders of these moments that depends essentially on the properties of self-similarity. The k^{th} product moment $m_k(\lambda)$ for a two-dimensional arbor with, for convenience, the same size parameter λ for both independent variables, is defined to be

$$\begin{aligned} m_k(\lambda) &= \int_{-\infty}^{\infty} dx\int_{-\infty}^{\infty} dyf(x,y,\lambda)\left|xy\right|^k \\ &= \lambda^{2h}\int_{-\infty}^{\infty} dx\int_{-\infty}^{\infty} dyf(x/\lambda,y/\lambda,1)\left|xy\right|^k \\ &= \lambda^{2h+2+2k}\int_{-\infty}^{\infty} d\xi\int_{-\infty}^{\infty} d\eta f(\xi,\eta,1)\left|\xi\eta\right|^k \\ &= \lambda^{2(h+1+k)}m_k(1) \end{aligned}$$

where the definition of self-similarity was used in the second line, the change of variables $\xi = x/\lambda$ and $\eta = y/\lambda$ was made in the third line, and $m_k(1)$ is the k^{th} moment for an arbor (or density function) whose size parameter has a value $\lambda = 1$. Notice that $m_k(1)$ is just a number (whose value depends on k) that is the same for all arbors with the same density function f. The discrete approximation of the moment function above is

$$m_k(\lambda) = \sum_j \left|xy\right|_j^k w_j(\lambda)$$

where the j is the arbor segment index, (x_j,y_j) is the center of the j^{th} segment, and $w_j(\lambda)$ [the discrete analog of the arbor density $f(x,y\lambda)$] is the length of the j^{th} segment. Many arbors have nearly circularly (or spherically) symmetric density functions, and for such circularly symmetric arbors (density functions), the odd-numbered moments would vanish if we had not taken the absolute value $|xy|$ above. We have therefore modified the usual definition of moments to the one we use here in order to ensure that the odd-numbered moments cannot vanish, even for circularly or spherically symmetric arbors. For even-numbered moments, our definition above coincides with the usual definition, which does not include the absolute values.

Because arbors do not come labeled with scale factors, we must have a way of estimating λ directly from the arbors themselves. The normalized second moment is

$$\sigma^2(\lambda) = \sqrt{m_2(\lambda)/m_0(\lambda)} = \sigma_x(\lambda)\sigma_y(\lambda)$$

(note that we have assumed separability in the third step) and, if we make use of the properties of $m_k(\lambda)$ for arbors that are self-similar, we find that

$$\sigma(\lambda) = \sqrt{\frac{\lambda^{h+3}}{\lambda^{h+1}}}\sigma(1) = \lambda$$

if $\sigma^2(1) = 1$ for the last step; this assignment is made here for notational simplicity but, in fact, we normalize any theoretical arbor density function we use so that $m_0(1)$ and $m_2(1)$ agree with the measured values. If λ is eliminated between this last equation and the expression above for $m_k(\lambda)$, the result $m_k(\lambda) = (\sigma^2(\lambda))^{h+1+k} m_k(1)$, (note that we still use λ as a label for the arbor even though it has been eliminated as a variable in the equation) or, after we take logarithms,

$$\log(m_k(\lambda)) = s(k)\log\left(\sigma^2(\lambda)\right) + l(k) \quad (1)$$

with $s(k)$ identified as

$$s(k) = k + (h+1) \quad (2)$$

and $l(k)$ just

$$l(k) = \log(m_k(1));$$

notice that $l(k)$ has a single value (that depends on k) for all arbors with the density function f. Equation 1 says that $\log(m_k)$ plotted against $\log(\sigma^2)$ should, for various values of λ, fall on a straight line if the function $f(x,y,\lambda)$ is self-similar; this is the first part of the test for self-similarity. The second part of the test, embodied in Equation 2, says the slope $s(k)$ as a function of k should also be a straight line with a slope of 1.

To calculate the intercepts $l(k)$ above, one must assume a functional form for the density function $f(x,y,\lambda)$. We chose a truncated Gaussian because at least some arbors have approximately circularly symmetric density functions that are nearly separable in Cartesian coordinates; a Gaussian (not truncated) is the only circularly symmetric function that is separable in Cartesian coordinates.

These same equations hold for functions of many variables, the only change being that, for example in three dimensions, $\lambda = (\lambda_x\lambda_y\lambda_z)$, where λ_x is the size parameter for the x direction, etc.

Intercepts for Self-Similarity Test (First Part)

When a double logarithmic plot of $m_k(\lambda)$ as a function of $\sigma_x\sigma_y$ is made, the intercept is $\log(m_k(1))$. If the $m_k(\lambda)$ are moments of a self-similar function, the intercept values, for $m_k(1)$ determine the functional form of that self-similar function. Because arbor branches terminate at the boundary of their convex hull area, the density function that describes them must vanish beyond that boundary. The goal here is to calculate the intercepts $\log(m_k(1))$ for several functional forms assuming that the boundary is circular. In the following, $m_k(1)$ will be denoted by the shorthand m_k.

If $\rho(x,y)$ is the density function, the intercepts in question are found from

$$m_k = \int\int_{-\infty}^{\infty} dxdy(xy)^k \rho(x,y).$$

The density function ρ is normalized so that $m_0 = 1$ and, to agree with data, $m_2 = 1$ is also required.

Truncated Gaussian in 2D

A truncated Gaussian is described by

$$\rho(x,\ y) = \begin{cases} \frac{1}{2\pi(1+\alpha)^2 C} e^{-\frac{x^2+y^2}{2(1+\alpha)^2}} & \text{if } \sqrt{x^2+y^2} \le R(1+\alpha) \\ 0 & \text{otherwise} \end{cases}$$

where

$$C = 1 - e^{-R^2/2}$$

and $\alpha(R)$ is a function of R that is chosen to make $m_2 = 1$. C normalizes the density function so that $m_0 = 1$.

To do business with this density function with a circular boundary, it is easier to switch to polar coordinates (r,θ). For this, we have

$$x = r\cos\theta$$

$$y = r\sin\theta$$

$$dxdy = rdrd\theta,$$

and the integral whose log gives the intercepts is

$$m_k = \frac{1}{2\pi(1+\alpha)^2 C}\overbrace{\int_0^{2\pi} d\theta(\cos\theta\ \sin\theta)^k}^{I_1(k)\equiv} \int_0^{R(1+\alpha)} drr^{2k+1} e^{\frac{r^2}{2(1+\alpha)^2}}.$$

The first integral $I_1(k)$ can be simplified to give

$$\begin{aligned} I_1(k) &= \int_0^{2\pi} d\theta(\cos\theta\ \sin\theta)^k \\ &= \frac{1}{2^k}\int_0^{2\pi} d\theta\ \sin^k\left(\overbrace{2\theta}^{\phi}\right) \\ &= \frac{1}{2^{k+1}}\int_0^{4\pi} d\phi\ \sin^k\phi \\ &= \tfrac{1}{2^k}\textstyle\int_0^{2\pi} d\phi\ \sin^k\phi. \end{aligned}$$

When $k = 0$, the value of the integral is $I_1(0) = 2\pi$, and when $k = 2$, the value is $I_1(2) = \pi/4$.

The second integral can also be simplified by a change of variables to give

$$\int_0^{R(1+\alpha)} drr^{2k} e^{-\overbrace{\frac{r^2}{2(1+\alpha)^2}}^{\xi=}} = (1+\alpha)^{2k+2} 2^k \int_0^{R^2/2} d\xi\xi^k e^{-\xi}.$$

For m_k, then, the result is

$$m_k = \frac{(1+\alpha)^{2k}}{2\pi C}\int_0^{2\pi} d\phi\ \sin^k\phi \int_0^{R^2/2} \xi^k e^{-\xi}.$$

When $k = 0$, the moment $m_0 = 1$ and the normalization factor C is calculated as

$$m_0 = 1 = \frac{1}{C}\int_0^{R^2/2} e^{-\xi} \text{ or } C = \int_0^{R^2/2} e^{-\xi} = 1 - e^{-R^2/2}.$$

The second condition for determining the normalization is $m_2 = 1$, and this is

$$m_0 = \frac{(1+\alpha)^4}{2C}\int_0^{R^2/2} d\xi\xi^2 e^{-\xi} = 1.$$

This means that $\alpha(R)$ can be determined by finding the root of the equation above (numerically) or by

$$\alpha = \sqrt[4]{\frac{2C}{\int_0^{R^2/2} d\xi\xi^2 e^{-\xi}}} - 1.$$

Uniform Density Inside a Circular Boundary in 2D

Another density function of interest is a "pill-box" function

$$\rho(x,y) = \begin{cases} \frac{1}{\pi R^2} & \text{if } \sqrt{x^2+y^2} \le R \\ 0 & \text{otherwise.} \end{cases},$$

a function with constant density within the arbor boundary. The change to polar coordinates here gives

$$m_k = \frac{1}{\pi R^2}\int_0^{2\pi} d\theta(\cos\theta\ \sin\theta)^k \int_0^R drr^{2k+1}.$$

This function is normalized so that $m_0 = 1$, but the only way to make $m_2 = 1$ is to select R so that

$$m_2 = \frac{R^6}{6 \cdot 4R^2} = \frac{R^4}{24} = 1 \text{ or } R = \sqrt[4]{24} = 2.213$$

Truncated Gaussian in 3D

The moments that are used to calculate the intercepts above for the 3D case are

$$m_{2k} = \int\int\int_{-\infty}^{\infty} dxdydz(xyz)^{2k}\rho(x,y,z).$$

To change from rectangular to spherical coordinates (ρ,θ,φ), the equations are

$$\begin{aligned} x &= r\cos\theta\sin\phi \\ y &= r\sin\theta\sin\phi \\ z &= r\cos\phi \\ dxdrdz &= r^2\sin\phi drd\theta d\phi. \end{aligned}$$

For a truncated Gaussian in 3D, then, the moment equation is

$$m_k = \frac{1}{(2\pi)^{3/2}(1+\alpha)^3 C}\int_0^{\pi} d\phi\cos^k\phi\sin^{2k+1}\phi \int_0^{2\pi} d\theta\cos^k\theta\sin^k\theta\cdot\int_0^{R(1+\alpha)} drr^{3k+2}e^{-\frac{r^2}{2(1+\alpha)^2}}.$$

As before, C is determined from the condition $m_0 = 1$, so that

$$1 = \frac{4\pi}{(2\pi)^{3/2}(1+\alpha)^3 C}\int_0^{R(1+\alpha)} drr^2 e^{-\overbrace{\frac{r2}{2(1+\alpha)^2}}^{\xi=}}$$

$$= \frac{4\pi(1+\alpha)^2}{(2\pi)^{3/2}(1+\alpha)^3 C}\int_0^{R^2/2} d\xi\sqrt{2\xi}(1+\alpha)e^{-\xi}$$

$$= \frac{2}{\sqrt{\pi}C}\int_0^{R^2/2} d\xi\xi^{1/2}e^{-\xi}$$

$$= \frac{2}{\sqrt{\pi}C}\left(\Gamma(1+1/2) - \Gamma(1+1/2, R^2/2)\right)$$

$$= \frac{1}{C}\left(1 - \frac{2\Gamma(1+1/2, R^2/2)}{\sqrt{\pi}}\right),$$

and C is therefore

$$= C\left(1 - \frac{2\Gamma(1+1/2, R^2/2)}{\sqrt{\pi}}\right).$$

The above used $\Gamma(1+1/2) = \sqrt{\pi}/2$.

Given the normalization constant C for the density function, the next job is to find the value of α that insures that the variance is 1. That is,

$$m_2 = 1$$

$$= \frac{\pi}{4(2\pi)^{\frac{3}{2}}(1+\alpha)^3 C}\overbrace{\int_0^{\pi} d\phi\cos^2\phi\sin^5\phi}^{\frac{16}{105}=}\int_0^{R(1+\alpha)} drr^8 e^{-\overbrace{\frac{r^2}{2(1+\alpha)^2}}^{\xi\equiv}}$$

$$= \frac{4\pi}{105(2\pi)^{\frac{3}{2}}(1+\alpha)C}\int_0^{R^2/2} d\xi\left(2(1+\alpha)^2\xi\right)^{3+1/2}e^{-\xi}$$

$$= \frac{16(1+\alpha)^6}{105\sqrt{\pi}C}\int_0^{R^2/2} d\xi\xi^{3+1/2}e^{-\xi}$$

$$= \frac{(1+\alpha)^6}{C}\left(1 - \frac{\Gamma(4+1/2, R^2/2)}{\Gamma(4+1/2)}\right).$$

Note that the relation

$$\Gamma(n+1/2) = \frac{(2n-1)!!}{2^n}\sqrt{\pi} \text{ so}$$

$$\Gamma(4+1/2) = \frac{105}{16}\sqrt{\pi}$$

was used. The second condition, then, means that α is determined by

$$\alpha = \sqrt[6]{\frac{C\Gamma(4+1/2)}{(\Gamma(4+1/2) - \Gamma(4+1/2, R^2/2))}} - 1.$$

Uniform Density Inside a Spherical Boundary

For a three-dimensional "pill-box" arbor with a density function that is constant inside the boundary with radius R, the k^{th} moment that determines the intercepts as above is

$$m_k = \frac{3}{4\pi R^3}\int_0^{\pi} d\phi\cos^k\phi\sin^{2k+1}\int_0^{2\pi} d\theta\cos^k\theta\sin^k\theta\int_0^R drr^{3k+2}.$$

From this equation, $m_0 = 1$. The value of R that makes $m_2 = 1$ then is gotten from

$$1 = \frac{3}{4\pi R^3}\overbrace{\int_0^{\pi} d\phi\cos^2\phi\sin^5\phi}^{16/105}\overbrace{\int_0^{2\pi} d\theta\cos^2\theta\sin^2\theta}^{\pi/4}\overbrace{\int_0^R drr^8}^{R^9/9} = \frac{R^6}{3\cdot 105}$$

so that the boundary should be at

$$\begin{aligned} R &= \sqrt[6]{315} \\ &= 2.608 \end{aligned}$$

SUPPLEMENTAL INFORMATION

Supplemental Information includes Supplemental Experimental Procedures: Separability and Self-Similar Functions and six figures and can be found with this article online at doi:10.1016/j.neuron.2010.02.013.

ACKNOWLEDGMENTS

This work was supported by the Howard Hughes Medical Institute. Part of the work was carried out at the Aspen Center for Physics and the Santa Fe Institute, and C.F.S. is grateful to these institutions for their hospitality and support.

Accepted: January 28, 2010
Published: April 14, 2010

REFERENCES

Barrenblatt, G.I. (1996). Scaling, Self-Similarity, and Intermediate Asymptotics, Volume 14 (Cambrdige, UK: Cambridge University Press).

Bertrand, N., Castro, D.S., and Guillemot, F. (2002). Proneural genes and the specification of neural cell types. Nat. Rev. Neurosci. *3*, 517–530.

Binzegger, T., Douglas, R.J., and Martin, K.A. (2004a). Axons in Cat Visual Cortex are Topologically Self-similar. Cereb. Cortex *15*, 152–165.

Binzegger, T., Douglas, R.J., and Martin, K.A. (2004b). A quantitative map of the circuit of cat primary visual cortex. J. Neurosci. *24*, 8441–8453.

Charron, F., and Tessier-Lavigne, M. (2007). The Hedgehog, TGF-beta/BMP and Wnt families of morphogens in axon guidance. Adv. Exp. Med. Biol. *621*, 116–133.

Chklovskii, D.B. (2004). Synaptic connectivity and neuronal morphology: two sides of the same coin. Neuron *43*, 609–617.

Clandinin, T.R., and Feldheim, D.A. (2009). Making a visual map: mechanisms and molecules. Curr. Opin. Neurobiol. *19*, 174–180.

Cline, H.T. (2001). Dendritic arbor development and synaptogenesis. Curr. Opin. Neurobiol. *11*, 118–126.

de Gennes, P.-G. (1979). Scaling Concepts in Polymer Physics (Ithaca, NY: Cornell University Press).

Flanagan, J.G., and Vanderhaeghen, P. (1998). The ephrins and Eph receptors in neural development. Annu. Rev. Neurosci. *21*, 309–345.

Gao, F.B. (2007). Molecular and cellular mechanisms of dendritic morphogenesis. Curr. Opin. Neurobiol. *17*, 525–532.

Hellwig, B. (2000). A quantitative analysis of the local connectivity between pyramidal neurons in layers 2/3 of the rat visual cortex. Biol. Cybern. *82*, 111–121.

Hsieh, J., and Gage, F.H. (2004). Epigenetic control of neural stem cell fate. Curr. Opin. Genet. Dev. *14*, 461–469.

Jaynes, E.T. (2003). Probability Theory: The Logic of Science (Cambridge, UK: Cambridge University Press).

Jessell, T.M. (2000). Neuronal specification in the spinal cord: inductive signals and transcriptional codes. Nat. Rev. Genet. *1*, 20–29.

Jimbo, H.C. (2004). Distribution characterization in a practical moment problem. Acta Math Univ. Comenianae *73*, 107–114.

Kalisman, N., Silberberg, G., and Markram, H. (2003). Deriving physical connectivity from neuronal morphology. Biol. Cybern. *88*, 210–218.

Krone, G., Mallot, H., Palm, G., and Schüz, A. (1986). Spatiotemporal receptive fields: a dynamical model derived from cortical architectonics. Proc. R Soc. Lond. B Biol. Sci. *226*, 421–444.

Lee, S., and Stevens, C.F. (2007). General design principle for scalable neural circuits in a vertebrate retina. Proc. Natl. Acad. Sci. USA *104*, 12931–12935.

Liley, D.T.J., and Wright, J.J. (1994). Intracortical connectivity of pyramidal and stellate cells: estimates of synaptic densities and coupling symmetry. Network Comput. Neural Syst. *5*, 175–189.

Louvi, A., and Artavanis-Tsakonas, S. (2006). Notch signalling in vertebrate neural development. Nat. Rev. Neurosci. *7*, 93–102.

Lübke, J., Roth, A., Feldmeyer, D., and Sakmann, B. (2003). Morphometric analysis of the columnar innervation domain of neurons connecting layer 4 and layer 2/3 of juvenile rat barrel cortex. Cereb. Cortex *13*, 1051–1063.

Luo, L., and Flanagan, J.G. (2007). Development of continuous and discrete neural maps. Neuron *56*, 284–300.

Niell, C.M., and Smith, S.J. (2005). Functional imaging reveals rapid development of visual response properties in the zebrafish tectum. Neuron *45*, 941–951.

Peters, A., and Payne, B.R. (1993). Numerical relationships between geniculocortical afferents and pyramidal cell modules in cat primary visual cortex. Cereb. Cortex *3*, 69–78.

Price, D.J., Kennedy, H., Dehay, C., Zhou, L., Mercier, M., Jossin, Y., Goffinet, A.M., Tissir, F., Blakey, D., and Molnár, Z. (2006). The development of cortical connections. Eur. J. Neurosci. *23*, 910–920.

Shepherd, G.M., Stepanyants, A., Bureau, I., Chklovskii, D., and Svoboda, K. (2005). Geometric and functional organization of cortical circuits. Nat. Neurosci. *8*, 782–790.

Sholl, A., and Uttley, A.M. (1953). Pattern discrimination and the visual cortex. Nature *171*, 387–388.

Stepanyants, A., Hof, P.R., and Chklovskii, D.B. (2002). Geometry and structural plasticity of synaptic connectivity. Neuron *34*, 275–288.

Stevens, C. (1982). Quantitative specification of neuronal form. Lect. Math Life Sci. *15*, 1–6.

Stevens, C.F. (2009). Darwin and Huxley revisited: the origin of allometry. J. Biology *8*, 14.11–14.17.

Tessier-Lavigne, M., and Goodman, C.S. (1996). The molecular biology of axon guidance. Science *274*, 1123–1133.

Uttley, A.M. (1955). The probability of neural connexions. Proc. Biol. Sci. B *144*, 229–240.

Uylings, H.B., and van Pelt, J. (2002). Measures for quantifying dendritic arborizations. Network *13*, 397–414.

Wässle, H., and Boycott, B.B. (1991). Functional architecture of the mammalian retina. Physiol. Rev. *71*, 447–480.

Wen, Q., Stepanyants, A., Elston, G.N., Grosberg, A.Y., and Chklovskii, D.B. (2009). Maximization of the connectivity repertoire as a statistical principle governing the shapes of dendritic arbors. Proc. Natl. Acad. Sci. USA *106*, 12536–12541.